Effect of cosolvent on protein stability: A theoretical investigation

ARTICLE *in* THE JOURNAL OF CHEMICAL PHYSICS · NOVEMBER 2014

Impact Factor: 2.95 · DOI: 10.1063/1.4895530

1 AUTHOR:

Tigran Chalikian
University of Toronto
96 PUBLICATIONS **3,246** CITATIONS

Effect of cosolvent on protein stability: A theoretical investigation

Tigran V. Chalikian

Citation: The Journal of Chemical Physics **141**, 22D504 (2014); doi: 10.1063/1.4895530
View online: http://dx.doi.org/10.1063/1.4895530
View Table of Contents: http://scitation.aip.org/content/aip/journal/jcp/141/22?ver=pdfcov
Published by the AIP Publishing

Effect of cosolvent on protein stability: A theoretical investigation

Tigran V. Chalikian[a)]
Department of Pharmaceutical Sciences, Leslie Dan Faculty of Pharmacy, University of Toronto, 144 College Street, Toronto, Ontario M5S 3M2, Canada

(Received 23 June 2014; accepted 19 August 2014; published online 17 September 2014)

We developed a statistical thermodynamic algorithm for analyzing solvent-induced folding/unfolding transitions of proteins. The energetics of protein transitions is governed by the interplay between the cavity formation contribution and the term reflecting direct solute-cosolvent interactions. The latter is viewed as an exchange reaction in which the binding of a cosolvent to a solute is accompanied by release of waters of hydration to the bulk. Our model clearly differentiates between the stoichiometric and non-stoichiometric interactions of solvent or co-solvent molecules with a solute. We analyzed the urea- and glycine betaine (GB)-induced conformational transitions of model proteins of varying size which are geometrically approximated by a sphere in their native state and a spherocylinder in their unfolded state. The free energy of cavity formation and its changes accompanying protein transitions were computed based on the concepts of scaled particle theory. The free energy of direct solute-cosolvent interactions were analyzed using empirical parameters previously determined for urea and GB interactions with low molecular weight model compounds. Our computations correctly capture the mode of action of urea and GB and yield realistic numbers for $(\partial\Delta G^{\circ}/\partial a_3)_{T,P}$ which are related to the m-values of protein denaturation. Urea is characterized by negative values of $(\partial\Delta G^{\circ}/\partial a_3)_{T,P}$ within the entire range of urea concentrations analyzed. At concentrations below ~1 M, GB exhibits positive values of $(\partial\Delta G^{\circ}/\partial a_3)_{T,P}$ which turn positive at higher GB concentrations. The balance between the thermodynamic contributions of cavity formation and direct solute-cosolvent interactions that, ultimately, defines the mode of cosolvent action is extremely subtle. A 20% increase or decrease in the equilibrium constant for solute-cosolvent binding may change the sign of $(\partial\Delta G^{\circ}/\partial a_3)_{T,P}$ thereby altering the mode of cosolvent action (stabilizing to destabilizing or *vice versa*). © *2014 AIP Publishing LLC*. [http://dx.doi.org/10.1063/1.4895530]

INTRODUCTION

Low molecular weight water-miscible cosolvents have the ability to increase or decrease the protein stability or they may be neutral.[1–3] There are several models that have been proposed to account for the effect of cosolvent on protein stability.[2,4–8] In particular, the local-bulk partitioning model interprets the preferential interaction coefficient in terms of the partition coefficient for the distribution of cosolvent between the local domain surrounding the protein molecule and the bulk domain of solution.[6,9,10] In the solvent exchange model, the mode of action of a specific cosolvent is considered to be governed by a complex interplay between the effects of cavity formation (the excluded volume effect) and direct solute-cosolvent interactions.[4,11] Solute-cosolvent interactions are viewed as an exchange reaction in which the binding of a cosolvent to protein is accompanied by release of water molecules to the bulk.[4,12–15]

The conformational energetics of a protein is determined, among others, by the differential free energies of cavity formation, ΔG_C, and direct solute-solvent interactions, ΔG_I, in the native and unfolded protein states. Scaled particle theory (SPT)-based computations reveal that the free energy of cavity formation, ΔG_C, generally, increases with an increase in the concentration of small cosolvents in solution.[16–19] Consequently, in the absence of sizeable interactions between protein groups and cosolvent molecules, a domain of reduced cosolvent concentration would be established in the immediate vicinity of the protein molecule in an attempt to diminish the unfavorable free energy of cavity formation, ΔG_C. The equilibrium will be attained at a local cosolvent concentration when any further decrease in the free energy of cavity formation is counterbalanced by the energetic penalty imposed by mixing entropy. However, should the direct solute-cosolvent interactions be sufficiently strong with the free energy of solute-cosolvent interactions, ΔG_I, offsetting or, even, exceeding ΔG_C in magnitude, the cosolvent depletion around the protein will become less pronounced or may, even, turn to preferential accumulation (binding). The balance between the ΔG_I and ΔG_C contributions is what makes a specific cosolvent neutral, preferentially bound, or preferentially excluded.

The native-to-unfolded transition (N-to-U) of a protein is accompanied by an increase in its solvent-accessible surface area which, in turn, leads to an increase in the free energy of cavity formation, ΔG_C, and a decrease in the free energy of solute-cosolvent interactions, ΔG_I. In the presence of a preferentially excluded cosolvent, the transition-induced increase in ΔG_C prevails over the decrease in ΔG_I which brings about stabilization of the native conformation. In contrast, a preferentially bound cosolvent stabilizes the unfolded conformation

a)Author to whom correspondence should be addressed. Electronic mail: chalikan@phm.utoronto.ca. Tel.: (416)946-3715. Fax: (416)978-8511.

of the protein by causing a larger transition-induced decrease in ΔG_I compared to an increase in ΔG_C.

We have previously introduced a statistical thermodynamic approach to analyzing interactions of cosolvents with proteins and protein groups.[20–24] The energetics of solute-cosolvent interactions has been evaluated from the cosolvent-dependent changes in volume and compressibility accompanying solute transfer from water to concentrated urea or glycine betaine (GB) solutions.[21–23] In those works, we have taken advantage of the modest contribution of the cavity term to the volumetric characteristics of small solutes' transfer from water to concentrated urea and glycine betaine solutions to quantify solvent exchange reactions in the vicinity of amino acid side chains and the peptide bond.[21–23]

In the current work, we further develop the statistical thermodynamic approach to model cosolvent-induced protein transitions. We apply this approach to characterizing the effect of the denaturant urea and the stabilizing osmolyte GB on the native/unfolded equilibria of model proteins which are geometrically approximated by a sphere in the native state and a spherocylinder in the unfolded state. With this approximation, we compute the effect of cosolvents on the free energy of cavity formation, ΔG_C, based on the concepts of scaled particle theory.[17,18] For evaluating the free energy of direct solute-cosolvent interactions, we derive a theoretical formalism based on the solvent-exchange model.[20–22] In the computations, we use experimentally determined equilibrium coefficients for interactions of urea and GB with low-molecular weight analogs of proteins.[21,23]

Despite geometric and physico-chemical simplifications introduced to the model, our analysis reveals a number of important insights into the molecular forces governing the effect of cosolvent on protein stability. Our conclusions are based on comparison of the computation results with the mode of action of urea and GB without interference of reconciliatory parameters. We do not use adjustable parameters that serve to close the gap between the experimental data and results of our model-dependent computations.

THEORETICAL MODEL

We consider a solute with identical and independent cosolvent-binding sites. Each cosolvent replaces r water molecules upon its binding to the solute. Under these simplifying assumptions, the concentration of a solute in a binary solvent containing water and cosolvent is given by the relationship[21]

$$[S] = [S]_0\left(1 + k_1 a_1^{\,r} + k_3 a_3\right)^{n/r}, \tag{1}$$

where n is the number of water molecules hydrating a solute in pure water (hydration number); $[S]_0$ is the concentration of dry unsolvated solute species; a_1 and a_3 are the activities of the principal solvent (water) and cosolvent, respectively; k_1 is the equilibrium constant for the reaction in which r water molecules bind to a dry cosolvent-binding site, $S_0 + rW \leftrightarrows SW_r$; and k_3 is the equilibrium constant for the reaction of association of a cosolvent with a dry cosolvent-binding site, $S_0 + C \leftrightarrows SC$.

If the protein population is in equilibrium between the native (N) and denatured (D) conformational species, Eq. (1) can be used to describe the concentration of the protein in each of its two conformations. Assuming that the affinities of water (k_1) and the cosolvent (k_3) for the binding sites do not change in the course of the folding/unfolding transition, one arrives at the relationships

$$[N] = [N]_0\left(1 + k_1 a_1^{\,r} + k_3 a_3\right)^{n_N/r} \tag{2a}$$

and

$$[D] = [D]_0\left(1 + k_1 a_1^{\,r} + k_3 a_3\right)^{n_D/r}, \tag{2b}$$

where $[N]_0$ and $[D]_0$ are the concentrations of the dry unsolvated native and denatured solute species, respectively; and n_N and n_D are the hydration numbers for the native and denatured states, respectively.

The equilibrium constant $K = [D]/[N]$ is given by the relationship

$$K = ([D]_0/[N]_0)\left(1 + k_1 a_1^{\,r} + k_3 a_3\right)^{(n_D - n_N)/r}. \tag{3}$$

A change in free energy accompanying protein denaturation is described by the following relationship:

$$\Delta G^\circ = -RT\ln K = -RT\ \ln([D]_0/[N]_0) - [(n_D - n_N)/r]\,RT\ \ln\left(1 + k_1 a_1^{\,r} + k_3 a_3\right). \tag{4}$$

The first term of Eq. (4), $-RT\ \ln([D]_0/[N]_0)$, is $\Delta\Delta G_C$, a change in free energy of cavity formation, ΔG_C, associated with the N-to-D transition. The second term describes the free energy of direct solute-solvent interactions. It is safe to assume that, in the second term, $1 \ll k_1 a_1^{\,r} + k_3 a_3$, since, in solution, the population of dry (unsolvated) binding sites is vanishingly small compared to the population of sites occupied by water or cosolvent. With this approximation, one arrives at the following:

$$\Delta G^\circ = \Delta\Delta G_C - [(n_D - n_N)/r]\,RT\ \ln\left(k_1 a_1^{\,r} + k_3 a_3\right). \tag{5}$$

Relationships similar to Eq. (5) in which the free energy of protein transition is considered within the context of cavity formation and solvation of protein groups have been reported previously.[4,11,17,18,25] There are two main distinctions between Eq. (5) and previous derivations, in particular, that described in Schellman's classical work.[4] Firstly, the cavity term, $\Delta\Delta G_C$, appears in Eq. (5) as a result of statistical thermodynamic treatment and not as an extra term added to account for an unaccounted expectation. Secondly, Eq. (5) can be used to describe an exchange reaction in which a cosolvent replaces any number of water molecules and not necessarily a single molecule.

The effect of cosolvent on protein stability is generally characterized by the m-value, $m = -(\partial\Delta G^\circ/\partial C_3)_{T,P}$, where C_3 is the molar concentration of cosolvent.[26] The derivative $(\partial\Delta G^\circ/\partial a_3)_{T,P}$ is related to m given $a_3 = \gamma_3 C_3$ (where γ_3 is the coefficient of cosolvent activity). In general, $(\partial\Delta G^\circ/\partial a_3)_{T,P} \neq (\partial\Delta G^\circ/\partial C_3)_{T,P}$, since $da_3 = \gamma_3 dC_3 + C_3 d\gamma_3$. However, for urea with $\gamma_3 \approx 1$ and weakly depending on concentration, $(\partial\Delta G^\circ/\partial a_3)_{T,P} \approx (\partial\Delta G^\circ/\partial C_3)_{T,P}$.[10]

The equation for $(\partial\Delta G^{\circ}/\partial a_3)_{T,P}$ can be derived by differentiating Eq. (5) with respect to cosolvent activity:

$$(\partial\Delta G^{\circ}/\partial a_3)_{T,P} = (\partial\Delta\Delta G_C/\partial a_3)_{T,P} - RT[(n_D - n_N)/r]\left[\left(ra_1^{r-1}(\partial a_1/\partial a_3\right)_{T,P} + (k_3/k_1))/(a_1^{r} + (k_3/k_1)a_3)\right]. \quad (6)$$

According to the Gibbs-Duhem equation, at constant P and T and a negligible solute concentration, $N_1 d\mu_1 + N_3 d\mu_3 = 0$ (where μ_1 and N_1 are the chemical potential and number of moles of the principal solvent, respectively; and μ_3 and N_3 are the chemical potential and number of moles of cosolvent, respectively), from which one obtains $N_1 d \ln a_1 = -N_3 d \ln a_3$ and, finally, $(\partial a_1/\partial a_3)_{T,P} = -(a_1/a_3)(N_3/N_1)$. By substituting this relationship in Eq. (6), one arrives at the following:

$$(\partial\Delta G^{\circ}/\partial a_3)_{T,P} = (\partial\Delta\Delta G_C/\partial a_3)_{T,P} - RT[(n_D - n_N)/r] \times\left[k/\left(a_1^{r} + ka_3\right)\right] + RT(n_D - n_N) \times\left[\left(a_1^{r}/a_3\right)/\left(a_1^{r} + ka_3\right)\right](N_3/N_1), \quad (7)$$

where $k = (k_3/k_1)$ is the equilibrium constant for a reaction in which a cosolvent molecule binds to a solute replacing r water molecules.

Given that $\Delta G^{\circ} = -RT \ln K$ and $d \ln a_3 = da_3/a_3$, Eq. (7) can be rearranged to the form:

$$(\partial \ln K/\partial \ln a_3)_{T,P} = -(1/RT)(\partial\Delta\Delta G_C/\partial \ln a_3)_{T,P} + [(n_D - n_N)/r][ka_3/(a_1^{r} + ka_3)] - (n_D - n_N)[a_1^{r}/(a_1^{r} + ka_3)](N_3/N_1). \quad (8)$$

Our derivations have implications for "osmotic stress" measurements in which equilibrium coefficient, K, is measured as a function of water activity, a_1, in an attempt to determine the number of water molecules released to or taken up from the bulk.[27] By differentiating lnK with respect to $\ln a_1$, one obtains the following relationship:

$$(\partial \ln K/\partial \ln a_1)_{T,P} = -(1/RT)(\partial\Delta\Delta G_C/\partial \ln a_1)_{T,P} + (n_D - n_N)[a_1^{r}/\left(a_1^{r} + ka_3\right)] - [(n_D - n_N)/r][ka_3/(a_1^{r} + ka_3)](N_1/N_3). \quad (9)$$

It is instructive to compare Eqs. (8) and (9) with $(\partial \ln K/\partial \ln a_3)_{T,P} = \Delta\Gamma_{23} = \Delta(\partial m_3/\partial m_2)_{T,P,\mu 3} = \Delta n_3 - (N_3/N_1)\Delta n_1$ and $(\partial \ln K/\partial \ln a_1)_{T,P} = \Delta\Gamma_{21} = \Delta(\partial m_1/\partial m_2)_{T,P,\mu 1} = \Delta n_1 - (N_1/N_3)\Delta n_3$, expressions which form the basis of the "osmotic stress" technique.[2,6,27–29] These expressions have been first derived by Tanford[30] who cautioned that, in contrast to preferential interaction parameters $\Delta\Gamma_{21}$ and $\Delta\Gamma_{23}$, excess numbers of solvent, Δn_1, and cosolvent, Δn_3, around the solute are not thermodynamic quantities. However, Δn_1 and Δn_2 can be rigorously defined in terms of the Kirkwood-Buff integrals if the solute-solvent and solute-cosolvent radial distribution functions are known.[7,8,31–34] Inspection of Eqs. (8) and (9) reveals that, in general, $\Delta n_1 \neq (n_D - n_N)[a_1^{r}/(a_1^{r} + ka_3)]$ and $\Delta n_3 \neq [(n_D - n_N)/r]\,[ka_3/(a_1^{r} + ka_3)]$. Clearly, $(\partial \ln K/\partial \ln a_3)_{T,P}$ and $(\partial \ln K/\partial \ln a_1)_{T,P}$ (and, hence, Δn_1 and Δn_3) probe not only the stoichiometric binding of water and cosolvent molecules to solute but also the solvation effect of cavity formation (excluded volume). The latter is related to preferential binding or exclusion of cosolvent molecules not directly interacting with the solute. Under such circumstances, a local increase or decrease in solvent-to-cosolvent ratio in the vicinity of the solute is related to and paid off by minimizing the free energy of cavity formation.

Even in the absence of any significant affinity between the solute and cosolvent molecules (when $k \sim 0$), the slope $(\partial \ln K/\partial \ln a_1)_{T,P}$ may not correspond in magnitude and, even, in sign to the stoichiometric number of water molecules, $(n_D - n_N)$, exchanged between the bulk and hydration phases should the free energy of cavity formation change with water activity. This notion is in concert with the careful definition of preferential hydration and a change in preferential hydration upon some process given by Timasheff.[35] It also attests to the limited applicability of models in which cosolvent-protein interactions are presented solely in terms of stoichiometric binding reactions. The "non-stoichiometric" contribution of cavity formation may be, simply, too large to be ignored.

Eq. (9) also explains the long standing observation that different preferentially excluded cosolvents may yield significantly different values of $(\partial \ln K/\partial \ln a_1)_{T,P}$ for the same reaction scrutinized by osmotic stress measurements.[36] For a preferentially excluded cosolvent with $k \sim 0$, Eq. (9) simplifies to $(\partial \ln K/\partial \ln a_1)_{T,P} = -(1/RT)(\partial\Delta\Delta G_C/\partial \ln a_1)_{T,P} + (n_D - n_N)$. While the second term of this relationship does not appear to depend on the identity of the cosolvent, the first (cavity) term, clearly, does thereby making $(\partial \ln K/\partial \ln a_1)_{T,P}$ and its ability to probe changes in hydration cosolvent-dependent.

In addition, Eq. (9) sheds light on the difference between volumetric and osmotic stress techniques in characterizing changes in hydration accompanying biomolecular reactions. Volumetric measurements which are, generally, performed in a one-component solvent (water) reflect solely the differential hydration $(n_D - n_N)$.[37] On the other hand, osmotic stress measurements which are performed in two-component solvents (water plus cosolvent) reflect all three terms of Eq. (9) or, if $k \sim 0$, the sum of the cavity term $-(1/RT)(\partial\Delta\Delta G_C/\partial \ln a_1)_{T,P}$ and $(n_D - n_N)$. Consequently, the hydration numbers yielded by volumetric and volumetric techniques may, generally, be distinct. A qualitatively similar conclusion has been drawn by Shimizu and co-authors[8,31–33] based on the application of the Kikwood-Buff theory to characterizing solute solvation in binary solvent-cosolvent mixtures.

RESULTS AND DISCUSSION

Computing free energy of cavity formation

We performed computations based on Eqs. (7) and (9) for hypothetical proteins of varying size for which the native and unfolded conformations are approximated, respectively, by a sphere and a spherocylinder of equal volume (Figure 1). The

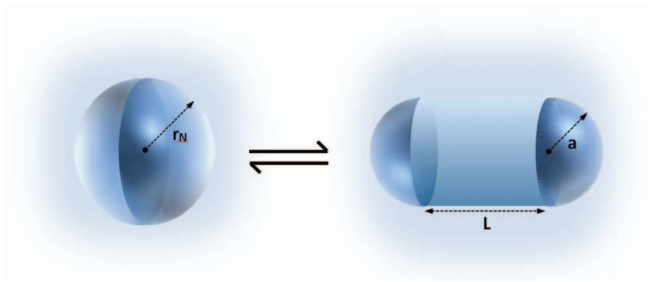

FIG. 1. Schematic representation of the equilibrium between the spherical native conformation and the spherocylindrical denatured conformation.

intrinsic volume, V_{MN}, and solvent accessible surface areas, S_{AN}, of a protein in its native (spherical) conformation are given by $V_{MN} = (4/3)\pi {r_N}^3$ and $S_{AN} = 4\pi(r_N + r_W)^2$, where r_N and r_W are the radii of the protein and water, respectively. The intrinsic volume, V_{MD}, and solvent accessible surface areas, S_{AD}, of the protein in the denatured (spherocylindrical) conformation are given by $V_{MD} = (4/3)\pi a^3 + \pi a^2 l$ and $S_{AD} = 4\pi(a + r_W)^2 + 2\pi l(a + r_W)$, respectively. Combining these relationships and taking into account that $V_{MN} = V_{MD} = V_M$, one obtains the following equation:

$$(2/3)a^4 + (8/3)r_W a^3 + \left(2{r_W}^2 - S_{AD}/2\pi\right)a^2 + (V_M/\pi)(a + r_W) = 0. \quad (10)$$

Eq. (10) can be used to calculate the spherocylindrical curvature, a, for any set of V_M and S_{AD}, while the cylindrical length, l, can be evaluated from $l = V_M/\pi a^2 - (4/3)a$. The free energies of cavity formation for the native, ΔG_{CN}, and unfolded, ΔG_{CD}, conformations can be calculated based on the concepts of SPT:[16–18]

$$\Delta G_{CN} = RT\{-\ln(1-\xi_3) + [6\xi_2/(1-\xi_3)]r_N + [12\xi_1/(1-\xi_3)]{r_N}^2 + \left[18{\xi_2}^2/(1-\xi_3)^2\right]{r_N}^2, \quad (11)$$

$$\Delta G_{CD} = RT\left\{-\ln(1-\xi_3) + [6\xi_2/(1-\xi_3)]a + [12\xi_1/(1-\xi_3)]a^2 + \left[18{\xi_2}^v/(1-\xi_3)^2\right]a^2 + [3\xi_2/2(1-\xi_3)]l + [6\xi_1/(1-\xi_3)]al + \left[9{\xi_2}^2/(1-\xi_3)^2\right]al\right\}, \quad (12)$$

where $\xi_i = (\pi/6)\sum_j N_A C_j {\sigma_j}^i$; N_A is Avogadro's number; C_j is the molar concentration of solution component j; and σ_j is the hard-sphere diameter of component j.[17,18]

In our computations, we use hard sphere diameters, σ_j, of 2.74, 4.41, and 6.08 Å for water, urea, and GB, respectively.[22] It should be noted, however, that SPT-based calculations critically depend on the specific choice of the geometric parameters of the solute and solvent components in Eqs. (11) and (12) as well as on the precise values of component concentrations C_i.[19] The problem of approximation of a complex molecular shape by simple geometric figures does not have any universal solution. Different approaches may yield significantly different parameters.[19] Another controversy is related to the choice of a specific pressure in SPT-based calculations.[19,38] Despite these uncertainties, SPT has proven to be a valuable tool in theoretical studies of solute-solvent interactions. While realizing the potential limitations of applying a simple hard sphere-based theory to studying complex water-based systems, we use in our analyses Eqs. (11) and (12) to calculate the free energies of cavity formation for the native, ΔG_{CN}, and unfolded, ΔG_{CD}, protein states.

TABLE I. Densities of urea solutions, ρ, and molar concentrations, C_1, and activities, a_1, of water at various urea concentrations of urea, C_3.

C_3 (M)	ρ (g cm^{-3})	C_1 (M)	a_1
0	0.997 047	55.34	1.000
2	1.028 580	50.42	0.962
4	1.059 045	45.43	0.919
6	1.088 645	40.41	0.871
8	1.117 403	35.37	0.816

Urea

Table I presents experimental data on the densities, ρ, of aqueous urea solutions (second column) at various cosolvent concentrations, C_3 (first column).[20] The third column of Table I presents the molar concentrations of water, C_1, at each urea concentration calculated as $C_1 = (\rho - M_3 C_3)/M_1$, where M_1 and M_3 are the molecular weights of water and urea, respectively. The coefficients of activity of water and urea are close to unity within the entire range of urea concentrations studied (0–8 M).[10,39] Therefore, the activity of water, a_1, is taken equal to its mole fraction, $\alpha_1 = C_1/(C_1 + C_3)$, while the activity of urea, a_3, is taken equal to its molar concentration, $a_3 = C_3$. The activity of water, a_1, is presented in the fourth column of Table I. For the use in our analytical computations, the empirical relationship between the activities of water, a_1, and urea, a_3, is approximated by $a_1 = \alpha_1 = 1 - 0.0174a_3 - 0.000696{a_3}^2$. The ratios $N_3/N_1 = C_3/C_1$ in Eq. (7) and $N_1/N_3 = C_1/C_3$ in Eq. (9) are given by $N_3/N_1 = (1-\alpha_1)/\alpha_1$ and $N_1/N_3 = \alpha_1/(1-\alpha_1)$, respectively.

We performed computations for hypothetical spherical proteins with radii of 10, 15, and 20 Å with each protein undergoing an unfolding transition to a spherocylindrical denatured state with a solvent accessible surface area, S_{AD}, twice as large as that of the native state, S_{AN}. In addition, for the 15 Å protein, we analyzed the transition to the denatured state with $S_{AD} = 3S_{AN}$. Table II lists the intrinsic volumes, V_M, solvent accessible surface areas, S_A, of the native state, and spherocylindrical curvatures, a, and cylindrical lengths, l, for the denatured state calculated with Eq. (10).

A note of caution is warranted here. Due to the ruggedness of the protein surface, a sphere is a poor approximation for the native state. For example, the intrinsic volume, V_M, and solvent accessible surface area, S_A, of lysozyme are 15 659 Å^3 and 6685 Å^2, respectively.[40] If the spherical approximation of lysozyme is based on V_M, the radius of the sphere is $r = (3V_M/4\pi)^{1/3} = 15.5$ Å, while, if S_A forms the basis of the approximation, the radius is much larger and equal to $r = (S_A/4\pi)^{1/2} = 23.1$ Å. The difference in radii reflects the ruggedness of the protein surface and reveals the shortcomings of the spherical approximation of a globular protein. Nevertheless, we proceed with the spherical approximation

TABLE II. Geometric parameters of the native (spherical) and denatured (spherocylindrical) conformations of three model proteins of varying radius, r_N. The spherocylindrical curvatures, a, and cylindrical lengths, l, for the 15 Å protein were determined for two denatured states with solvent accessible surface areas, S_{AD}, double and triple of that of the native state, S_{AN}.

			$S_{AD} = 2S_{AN}$		$S_{AD} = 3S_{AN}$	
r_N (Å)	V_M (Å^3)	S_{AN} (Å^2)	a (Å)	l (Å)	a (Å)	l (Å)
10	4189	1257	4.75	52.79		
15	14 137	2827	6.48	98.53	4.48	128.23
20	33 509	5026	8.21	147.38		

and concentrate on qualitative rather than quantitative conclusions emerging from our analysis.

We used Eqs. (11) and (12) to calculate changes in the free energy of cavity formation, $\Delta\Delta G_C = \Delta G_{CD} - \Delta G_{CN}$, accompanying unfolding transitions of the 10, 15, and 20 Å proteins. Table III presents results of these computations. Note that, in all of our calculations, $\Delta\Delta G_C$ increases with an increase in urea concentration making the $(\partial\Delta\Delta G_C/\partial a_3)_{T,P}$ term in Eq. (7) and the $-(1/RT)(\partial\Delta\Delta G_C/\partial \ln a_1)_{T,P}$ term in Eq. (9) both positive.

With $\Delta\Delta G_C$ calculated, we proceed to compute the urea-dependences of $(\partial\Delta G^\circ/\partial a_3)_{T,P}$ and $(\partial \ln K/\partial \ln a_1)_{T,P}$ using Eqs. (7) and (9). We analyze $(\partial\Delta G^\circ/\partial a_3)_{T,P}$ instead of $(\partial \ln K/\partial \ln a_3)_{T,P}$, since the former is more directly related to m-value, $m = -(\partial\Delta G^\circ/\partial C_3)_{T,P}$, a fundamental, empirically determinable property of solvent-induced protein denaturation. The numbers of water molecules hydrating the native, n_N, and denatured, n_D, protein states are taken equal to the ratio of their respective solvent accessible surface areas (S_{AN} or S_{AD}) to 9 Å^2, the cross-sectional area of a water molecule. The number of water molecules released to the bulk from the hydration shell of a protein upon urea binding, r, equals 2.[20] The equilibrium constant, k, is taken equal to 0.1 M, the rounded average value of k evaluated for interaction of urea with small protein analogs.[21] However, as shown below, results of calculations strongly depend on the value of k used in the analysis.

Figures 2 and 3 show, respectively, the urea dependences of $(\partial\Delta G^\circ/\partial a_3)_{T,P}$ and $(\partial \ln K/\partial \ln a_1)_{T,P}$ for the unfolding transitions of the 10, 15, and 20 Å proteins to the denatured state with $S_{AD} = 2\ S_{AN}$. The insets in Figures 2 and 3 compare,

TABLE III. Changes in free energy of cavity formation, $\Delta\Delta G_C$ (kcal mol^{-1}), accompanying denaturation of the 10, 15, and 20 Å proteins at various urea concentrations, C_3.

C_3 (M)	10 Å[a]	15 Å[a]	15 Å[b]	20 Å[a]
0	62.1	162.4	348.4	310.6
2	64.6	169.0	362.4	323.0
4	67.3	175.9	377.3	336.3
6	70.0	183.2	392.9	350.2
8	72.9	190.8	409.4	364.9

[a]The solvent accessible surface area of the denatured state, S_{AD}, is double of that of the native state, S_{AN}.
[b]The solvent accessible surface area of the denatured state, S_{AD}, is triple of that of the native state, S_{AN}.

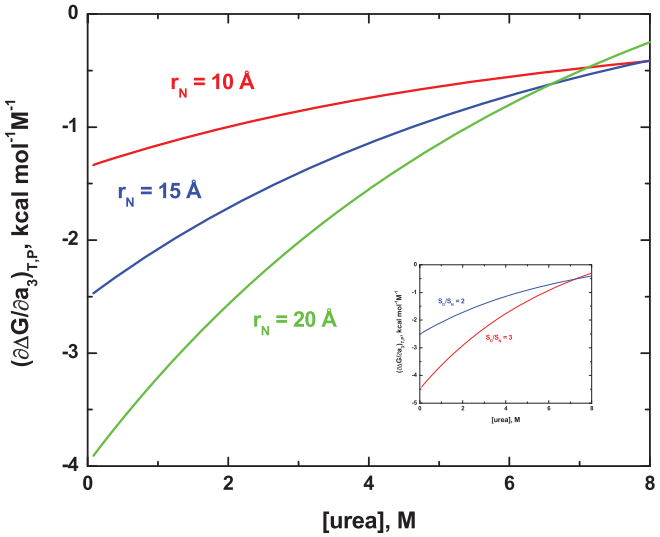

FIG. 2. Urea dependences of $(\partial\Delta G^\circ/\partial a_3)_{T,P}$ for the 10 (red), 15 (blue), and 20 (green) Å proteins for the unfolding transitions to the denatured state with $S_{AD} = 2\ S_{AN}$. The inset compares the urea dependences of $(\partial\Delta G^\circ/\partial a_3)_{T,P}$ determined for the transition of the 15 Å protein from the native state to the denatured state with S_{AD} equal to $2S_{AN}$ (blue) and $3S_{AN}$ (red).

respectively, the urea dependences of $(\partial\Delta G^\circ/\partial a_3)_{T,P}$ and $(\partial \ln K/\partial \ln a_1)_{T,P}$ calculated for the transition of the 15 Å protein from the native state to the denatured states with S_{AD} of $2S_{AN}$ and $3S_{AN}$. Since the coefficient of activity of urea in aqueous solution is around unity and, hence, $a_3 \approx C_3$, our calculated values of $(\partial\Delta G^\circ/\partial a_3)_{T,P}$ nearly coincide with the negative m-values $[m = -(\partial\Delta G^\circ/\partial C_3)_{T,P}]$.

Inspection of Figure 2 reveals a number of important observations. Firstly, for all proteins, the values of $(\partial\Delta G^\circ/\partial a_3)_{T,P}$ are negative within the entire range of urea concentrations considered here, an observation consistent

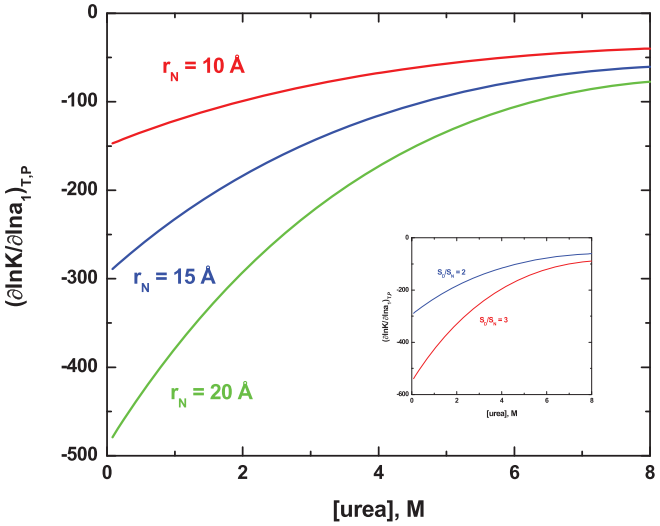

FIG. 3. Urea dependences of $(\partial \ln K/\partial \ln a_1)_{T,P}$ for the 10 (red), 15 (blue), and 20 (green) Å proteins for the unfolding transitions to the denatured state with $S_{AD} = 2\ S_{AN}$. The inset compares the urea dependences of $(\partial \ln K/\partial \ln a_1)_{T,P}$ determined for the transition of the 15 Å protein from the native state to the denatured state with S_{AD} equal to $2S_{AN}$ (blue) and $3S_{AN}$ (red).

with the denaturing nature of urea. Secondly, despite the hypothetical nature of the proteins analyzed, the range of the computed values of $(\partial\Delta G^{\circ}/\partial a_3)_{T,P}$ are numerically similar to the experimental range of m-values observed for urea-induced protein unfolding (on the order of ~2 kcal mol^{-1} M^{-1}).[41,42] The observed similarity lends credence to the theoretical framework and the specific parameters used in our analyses. Thirdly, in contrast to experimental observations,[26,42–44] the values of $(\partial\Delta G^{\circ}/\partial a_3)_{T,P}$ are not constant but increase nonlinearly as the concentration of urea increases from 0 to 8 M. The observed variability of $(\partial\Delta G^{\circ}/\partial a_3)_{T,P}$ may reflect the geometric approximations of the folded and unfolded protein states, an oversimplification which may not be warranted. In addition, the denatured state of the protein may become more unfolded (with a concomitant increase in the solvent accessible surface area of the unfolded state) at the concentrations of urea increases.[3] While this possibility is not accounted for by the theoretical model used in our analyses, the inset in Figure 2 suggests that $(\partial\Delta G^{\circ}/\partial a_3)_{T,P}$ strongly depends on ΔS_A.

Inspection of Figure 3 reveals that, for all proteins, $(\partial \ln K/\partial \ln a_1)_{T,P}$ increases hyperbolically as the urea concentration increases from 0 to 8 M while remaining negative within the entire range of urea concentrations. The negative sign of $(\partial \ln K/\partial \ln a_1)_{T,P}$ suggests that the effects of cavity formation and urea binding [the first and third terms of Eq. (9)] prevail over the effect of uptake of water accompanying protein unfolding [the second term of Eq. (9)]. This observation characterizes urea as a preferentially bound compound, a precondition for a denaturing cosolvent.

Further inspection of Figures 2 and 3 reveals that $(\partial\Delta G^{\circ}/\partial a_3)_{T,P}$ and $(\partial \ln K/\partial \ln a_1)_{T,P}$ correlate to changes in solvent accessible surface area, $\Delta S_A = S_{AD} - S_{AN}$. To make this point more obvious, Figure 4 presents the values of $(\partial\Delta G^{\circ}/\partial a_3)_{T,P}$ normalized per ΔS_A. As is seen from comparison of Figures 2 and 4, the normalized $[\Delta(\partial\Delta G^{\circ}/\partial a_3)_{T,P}/\Delta S_A]$-*versus*-urea plots run within 15–20% of each other, while the original $(\partial\Delta G^{\circ}/\partial a_3)_{T,P}$-*versus*-urea plots are manifold different. A similar observation can be made for the normalized $[\Delta(\partial \ln K/\partial \ln a_1)_{T,P}/\Delta S_A]$-*versus*-urea plots (data not shown). These results are consistent with the experimentally determined linear correlations between the m-value of a urea-induced unfolding transition and the accompanying change in solvent-accessible surface area, ΔS_A.[41]

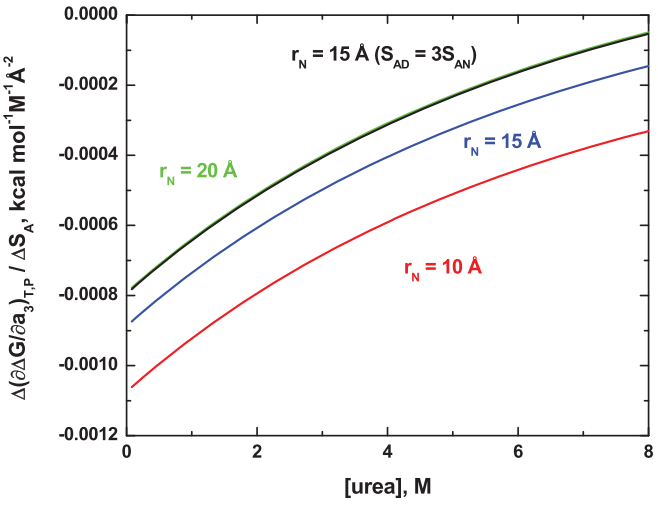

FIG. 4. The values of $(\partial\Delta G^{\circ}/\partial a_3)_{T,P}$ normalized per change in solvent accessible surface area, ΔS_A, plotted as a function of urea for the 10 (red), 15 (blue), and 20 (green) Å proteins denaturing to a state with $S_{AD} = 2\,S_{AN}$.

It is easy to understand the origins of the proportionality of $(\partial\Delta G^{\circ}/\partial a_3)_{T,P}$ and $\Delta(\partial \ln K/\partial \ln a_1)_{T,P}$ to ΔS_A by examining Eqs. (7) and (9). The second and third terms of Eqs. (7) and (9) are proportional to the differential number of water molecules solvating the denatured and native conformations, $(n_D - n_N)$, which, in turn, is proportional to the differential solvent accessible surface area, ΔS_A. On the other hand, numerical analysis of the data on $\Delta\Delta G_C$ presented in Table III reveals that the differential free energy of cavity of formation, $\Delta\Delta G_C$, is also roughly proportional to ΔS_A. By extension, the derivatives $(\partial\Delta\Delta G_C/\partial a_3)_{T,P}$ and $(\partial\Delta\Delta G_C/\partial \ln a_1)_{T,P}$ [the first terms in Eqs. (7) and (9)] are also linear functions of ΔS_A. Thus, all terms of Eqs. (7) and (9) are roughly proportional to ΔS_A, thereby collectively rendering $(\partial\Delta\Delta G_C/\partial a_3)_{T,P}$ and $(\partial \ln K/\partial \ln a_1)_{T,P}$ linear functions of ΔS_A.

Glycine betaine

Table IV shows the densities, ρ, of GB solutions, the molar concentrations of water, C_1, and its mole fraction, $\alpha_1 = C_1/(C_1 + C_3)$, as well as the activities of water, a_1, and GB, a_3, as a function of GB concentration, C_3. To be used in Eqs. (7) and (9), a_1 and a_3 are approximated by empirical relationships $a_1 = 1 - 0.00463\,C_3 - 0.01214\,C_3^2$ and $a_3 = -0.5 + 0.5\exp(C_3/0.86)$, respectively. Analogous to urea, the ratio N_3/N_1 in Eq. (7) is given by $N_3/N_1 = (1 - \alpha_1)/\alpha_1$, while the ratio N_1/N_3 in Eq. (9) is given by $N_1/N_3 = \alpha_1/(1 - \alpha_1)$. The mole fraction of water, α_1, in Table IV is approximated by $\alpha_1 = 1 - 0.0163\,C_3 - 0.0025\,C_3^2$.

Table V presents results of our SPT-based calculations of the differential free energy of cavity formation, $\Delta\Delta G_C$, for the 10, 15, and 20 Å proteins in their native and the denatured states with $S_{AD} = 2S_{AN}$. For the 15 Å protein, Table V also lists the differential $\Delta\Delta G_C$ values calculated for the native and the denatured state with $S_{AD} = 3S_{AN}$. Analogous to urea, $\Delta\Delta G_C$ increases with an increase in GB concentration resulting in positive $(\partial\Delta\Delta G_C/\partial a_3)_{T,P}$ term in Eq. (7) and $-(1/RT)(\partial\Delta G_C/\partial \ln a_1)_{T,P}$ term in Eq. (9).

TABLE IV. Activities of water, a_1, and GB, a_3, densities of GB solutions, ρ, and molar concentrations, C_1, and mole fractions, α_1, of water at various GB concentrations, C_3.

C_3 (M)	a_1 [a]	a_3 [a]	ρ (g cm^{-3}) [b]	C_1 (M)	α_1
0	1.000	0	0.997 047	55.34	1.000
1	0.976	1.62	1.016 001	49.89	0.980
2	0.939	5.65	1.035 113	44.46	0.957
3	0.880	16.59	1.054 651	39.05	0.929
4	0.782	52.61	1.074 620	33.65	0.894

[a]From Ref. 10.
[b]From Ref. 23.

TABLE V. Changes in free energy of cavity formation, $\Delta\Delta G_C$ (kcal mol^{-1}), accompanying denaturation of the 10, 15, and 20 Å proteins at various GB concentrations, C_3.

C_3 (M)	10 Å[a]	15 Å[a]	15 Å[b]	20 Å[a]
0	62.1	162.4	348.4	310.6
1	64.9	169.7	364.0	324.4
2	68.2	178.3	382.6	340.9
3	72.2	188.7	404.9	360.8
4	77.0	201.3	431.9	385.0

[a]The solvent accessible surface area of the denatured state, S_{AD}, is double of that of the native state, S_{AN}.
[b]The solvent accessible surface area of the denatured state, S_{AD}, is triple of that of the native state, S_{AN}.

We compute the GB-dependences of $(\partial\Delta G^\circ/\partial a_3)_{T,P}$ and $(\partial \ln K/\partial \ln a_1)_{T,P}$ using Eqs. (7) and (9). The number of water molecules released to the bulk from the hydration shell of a protein upon its association with a GB molecule, r, is 4.[23] The equilibrium constant, k, is taken equal to 0.15 M, the rounded average of the values of k evaluated for interaction of GB with small protein analogs,[23] although, for whole proteins, the values of k are somewhat larger.[24]

Figures 5 and 6 show, respectively, the GB dependences of $(\partial\Delta G^\circ/\partial a_3)_{T,P}$ and $(\partial \ln K/\partial \ln a_1)_{T,P}$ for the 10, 15, and 20 Å proteins for their transitions to the denatured states with $S_{AD} = 2\ S_{AN}$. The insets in Figures 5 and 6 compare, respectively, the GB dependences of $(\partial\Delta G^\circ/\partial a_3)_{T,P}$ and $(\partial \ln K/\partial \ln a_1)_{T,P}$ determined for the transitions of the 15 Å protein from the native state to the denatured state with S_{AD} equal to $2S_{AN}$ and $3S_{AN}$. Inspection of Figure 5 reveals that, for each protein, $(\partial\Delta G^\circ/\partial a_3)_{T,P}$ is positive at GB concentrations below ~1 M while becoming negative at higher concentrations. This result suggests that, while stabilizing proteins at low concentrations, GB exerts a destabilizing influence at high concentrations.

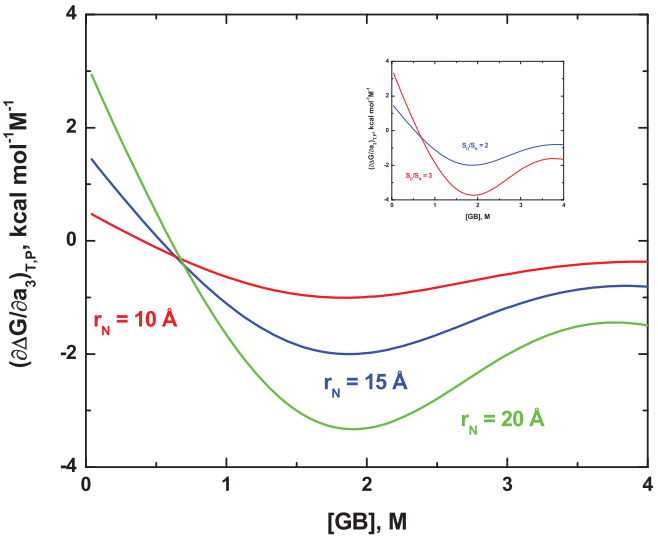

FIG. 5. GB dependences of $(\partial\Delta G^\circ/\partial a_3)_{T,P}$ for the 10 (red), 15 (blue), and 20 (green) Å proteins for the unfolding transitions to the denatured state with $S_{AD} = 2\ S_{AN}$. The inset compares the GB dependences of $(\partial\Delta G^\circ/\partial a_3)_{T,P}$ determined for the transition of the 15 Å protein from the native state to the denatured state with S_{AD} equal to $2S_{AN}$ (blue) and $3S_{AN}$ (red).

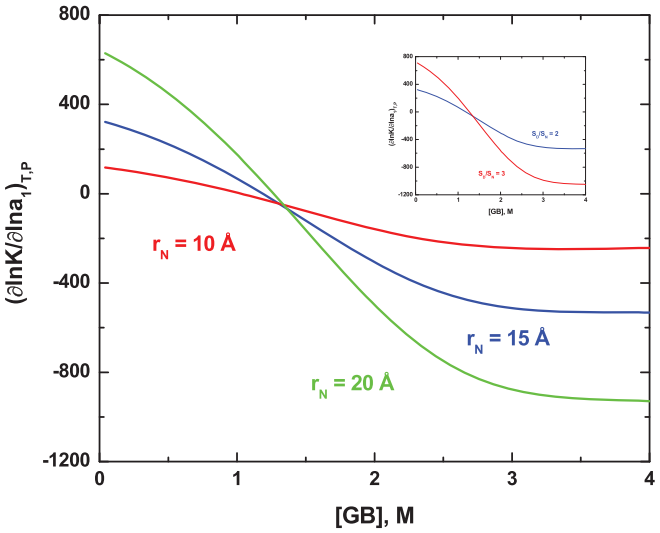

FIG. 6. GB dependences of $(\partial \ln K/\partial \ln a_1)_{T,P}$ for the 10 (red), 15 (blue), and 20 (green) Å proteins for the unfolding transitions to the denatured state with $S_{AD} = 2\ S_{AN}$. The inset compares the GB dependences of $(\partial \ln K/\partial \ln a_1)_{T,P}$ determined for the transition of the 15 Å protein from the native state to the denatured state with S_{AD} equal to $2S_{AN}$ (blue) and $3S_{AN}$ (red).

This intriguing result is in qualitative agreement with the presence of the maxima in the GB-dependences of the melting temperatures, T_M, of ribonuclease A and lysozyme within 3–4 M GB as measured by Bolen and co-workers.[45] In addition, it is consistent with the analysis of the distribution of GB in the vicinity of lac1 helix-turn-helix (HTH) DNA binding domain presented by Felitsky and Record.[10] These authors predict a reversal of the stabilizing effect of GB at high concentrations. In particular, they have found that the local-bulk partition coefficient, K_P, of GB near the protein is smaller than 1 between 0 and ~4 M GB but intersects the unity line and exceeds 1 at higher cosolvent concentrations.[10] It is remarkable that our simple, generalized model captures the reversal of the GB action at higher cosolvent concentrations. The quantitative difference in the onset of the reversal (~1 M versus ~4 M) is not unexpected in light of the many geometric and physicochemical simplifications that have been introduced when developing the model.

Inspection of Figure 6 reveals that, for all proteins, $(\partial \ln K/\partial \ln a_1)_{T,P}$ parallels the sign-reversal behavior of $(\partial\Delta G^\circ/\partial a_3)_{T,P}$. The values of $(\partial \ln K/\partial \ln a_1)_{T,P}$ are positive below ~1.5 M GB becoming negative at higher concentrations. Thus, GB is preferentially excluded at low concentrations gradually changing to preferentially bound as the cosolvent concentration increases. Analysis of the data in Table V in conjunction with Eq. (9) suggests that the cavity term, $-(1/RT)(\partial\Delta\Delta G_C/\partial \ln a_1)_{T,P}$, is positive favoring an increase in preferential hydration (cosolvent exclusion). In contrast, the sum of the interaction terms (second and third) of Eq. (9) is negative due to considerable solute-cosolvent interactions thereby favoring preferential binding of GB. Thus, the sign and the magnitude of $(\partial \ln K/\partial \ln a_1)_{T,P}$ at specific GB concentrations are determined by a subtle balance between the cavity and interaction contributions which, ultimately, defines the mode of cosolvent action.

The role of direct solute-cosolvent interactions

Based on the current results as well as our published data,[21–24] the mode of action of a specific cosolvent on the folding/unfolding equilibria of proteins is governed by the interplay between the thermodynamics of cavity formation and direct solute-cosolvent interactions. To probe the extent of the influence of solute-solvent interactions on the energetics of protein transitions, we use Eq. (7) to perform computations of $(\partial\Delta G^{\circ}/\partial a_3)_{T,P}$ for the 15 Å protein with $S_{AD} = 2S_{AN}$ in urea and GB using equilibrium constants, k, which vary by 20%. Results of these computations are presented in Figures 7(a) and 7(b). Inspection of Figures 7(a) and 7(b) reveals that a 20% change in k may alter not only the magnitude but also the sign of $(\partial\Delta G^{\circ}/\partial a_3)_{T,P}$ thereby altering the nature (stabilizing or destabilizing) of the cosolvent. These observations are consistent with a picture in which a slight increase or decrease in k for a specific atomic group may flip the mode of action of a specific cosolvent from preferentially excluded to preferentially bound and vice versa. The notion is in qualitative agreement with results from the Record group that suggest that urea and GB are preferentially excluded from certain functional groups while being preferentially bound to other groups.[46–49]

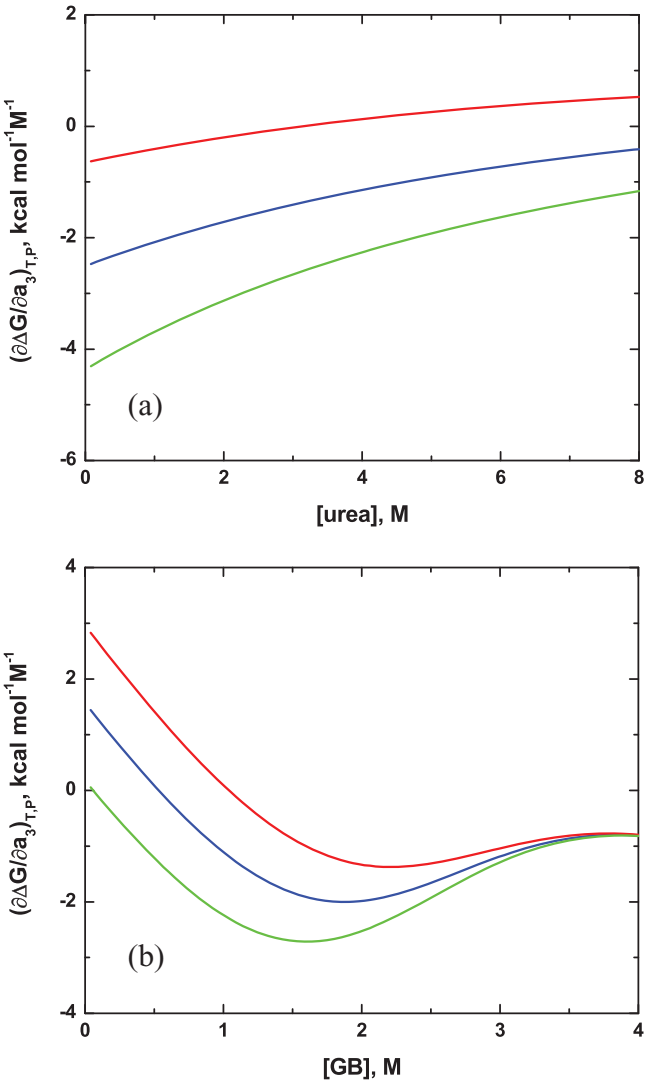

FIG. 7. (a) Urea dependences of $(\partial\Delta G^{\circ}/\partial a_3)_{T,P}$ calculated for the 15 Å protein ($S_{AD} = 2\,S_{AN}$) using the equilibrium constants, k, in Eq. (7) of 0.08 (red), 0.10 (blue), and 0.12 (green) M; (b) GB dependences of $(\partial\Delta G^{\circ}/\partial a_3)_{T,P}$ calculated for the 15 Å protein ($S_{AD} = 2\,S_{AN}$) using the equilibrium constants, k, in Eq. (7) of 0.12 (red), 0.15 (blue), and 0.18 (green) M.

CONCLUSIONS

A simple statistical thermodynamic model was developed and used to analyze cosolvent-induced protein transitions. In the model, the transition thermodynamics is governed by the balance between the thermodynamics of cavity formation and that of direct solute-cosolvent interactions. Solute-cosolvent interactions are treated as an exchange reaction in which the binding of a cosolvent is accompanied by release of water molecules from the solute's hydration shell to the bulk. The free energy of cavity formation is evaluated based on the concepts of scaled particle theory with protein approximated by a sphere in the native state and a spherocylinder in the unfolded state.

Our computations correctly capture the mode of action of urea and GB and yield realistic numbers for $(\partial\Delta G^{\circ}/\partial a_3)_{T,P}$ which are related to the m-values of protein denaturation. Urea is characterized by negative values of $(\partial\Delta G^{\circ}/\partial a_3)_{T,P}$ within the entire range of urea concentrations analyzed. At concentrations below ~1 M, GB exhibits positive values of $(\partial\Delta G^{\circ}/\partial a_3)_{T,P}$ which turn negative at higher GB concentrations. In contrast to experimental observations, the values $(\partial\Delta G^{\circ}/\partial a_3)_{T,P}$ for urea are not constant but nonlinearly increase with an increase in its concentration. The discrepancy between the experimental data and our computation results may be related to the geometric and physico-chemical simplifications introduced into the model.

Our results suggest that the balance between the thermodynamic contributions of cavity formation and direct solute-cosolvent interactions that, ultimately, defines the mode of cosolvent action is extremely subtle. A 20% increase or decrease in the equilibrium constant for solute-cosolvent interactions may change the sign of $(\partial\Delta G^{\circ}/\partial a_3)_{T,P}$ thereby altering the mode of cosolvent action (stabilizing to destabilizing or *vice versa*).

Further improvement of the model is related to a more realistic consideration of the effect of cavity formation, the use of individual equilibrium constants, k, for atomic groups of varying chemical nature, and the possibility of accounting for an increase in the degree of protein unfolding with an increase in cosolvent concentration.

ACKNOWLEDGMENTS

This work was supported by a grant from the Natural Sciences and Engineering Research Council of Canada. I thank Dr. Jens Völker and Dr. Giuseppe Graziano and Mr. Yuen Lai Shek for many useful discussions.

[1]S. N. Timasheff, Annu. Rev. Biophys. Biomol. Struct. **22**, 67 (1993).
[2]S. N. Timasheff, Adv. Protein Chem. **51**, 355 (1998).
[3]D. R. Canchi and A. E. Garcia, Annu. Rev. Phys. Chem. **64**, 273 (2013).
[4]J. A. Schellman, Biophys. J. **85**, 108 (2003).

[5]M. Auton and D. W. Bolen, Methods Enzymol. **428**, 397 (2007).
[6]M. T. Record and C. F. Anderson, Biophys. J. **68**, 786 (1995).
[7]V. Pierce, M. Kang, M. Aburi, S. Weerasinghe, and P. E. Smith, Cell Biochem. Biophys. **50**, 1 (2008).
[8]S. Shimizu, Proc. Natl. Acad. Sci. U. S. A. **101**, 1195 (2004).
[9]E. S., Courtenay, M. W. Capp, R. M. Saecker, and M. T. Record, Jr., Proteins, **41**(Suppl. 4), 72 (2000).
[10]D. J. Felitsky and M. T. Record, Biochemistry **43**, 9276 (2004).
[11]P. R. Davis-Searles, A. J. Saunders, D. A. Erie, D. J. Winzor, and G. J. Pielak, Annu. Rev. Biophys. Biomol. Struct. **30**, 271 (2001).
[12]J. A. Schellman, Biopolymers **26**, 549 (1987).
[13]J. A. Schellman, Biophys. Chem. **45**, 273 (1993).
[14]J. A. Schellman, Annu. Rev. Biophys. Biophys. Chem. **16**, 115 (1987).
[15]J. A. Schellman, Biopolymers **34**, 1015 (1994).
[16]R. A. Pierotti, Chem. Rev. **76**, 717 (1976).
[17]G. Graziano, Phys. Chem. Chem. Phys. **13**, 17689 (2011).
[18]G. Graziano, Phys. Chem. Chem. Phys. **13**, 12008 (2011).
[19]K. E. S. Tang and V. A. Bloomfield, Biophys. J. **79**, 2222 (2000).
[20]S. Lee and T. V. Chalikian, J. Phys. Chem. B **113**, 2443 (2009).
[21]S. Lee, Y. L. Shek, and T. V. Chalikian, Biopolymers **93**, 866 (2010).
[22]T. V. Chalikian, Biophys. Chem. **156**, 3 (2011).
[23]Y. L. Shek and T. V. Chalikian, J. Phys. Chem. B **115**, 11481 (2011).
[24]Y. L. Shek and T. V. Chalikian, Biochemistry **52**, 672 (2013).
[25]A. Ben-Naim, J. Chem. Phys. **137**, 235102 (2012).
[26]C. N. Pace and K. L. Shaw, Proteins **41**(Suppl. 4), 1 (2000).
[27]V. A. Parsegian, R. P. Rand, and D. C. Rau, Methods Enzymol. **259**, 43 (1995).
[28]S. N. Timasheff, Biochemistry **31**, 9857 (1992).
[29]V. A. Parsegian, R. P. Rand, and D. C. Rau, Proc. Natl. Acad. Sci. U. S. A. **97**, 3987 (2000).
[30]C. Tanford, J. Mol. Biol. **39**, 539 (1969).
[31]S. Shimizu and C. L. Boon, J. Chem. Phys. **121**, 9147 (2004).
[32]S. Shimizu and N. Matubayasi, Chem. Phys. Lett. **420**, 518 (2006).
[33]S. Shimizu and N. Matubayasi, J. Phys. Chem. B **118**, 3922 (2014).
[34]I. L. Shulgin and E. Ruckenstein, J. Chem. Phys. **123**, 054909 (2005).
[35]S. N. Timasheff, Biochemistry **41**, 13473 (2002).
[36]D. Harries, D. C. Rau, and V. A. Parsegian, J. Am. Chem. Soc. **127**, 2184 (2005).
[37]T. V. Chalikian and K. J. Breslauer, Curr. Opin. Struct. Biol. **8**, 657 (1998).
[38]S. Shimizu, M. Ikeguchi, S. Nakamura, and K. Shimizu, J. Chem. Phys. **110**, 2971 (1999).l
[39]O. Miyawaki, A. Saito, T. Matsuo, and K. Nakamura, Biosci., Biotechnol., Biochem. **61**, 466 (1997).
[40]T. V. Chalikian, M. Totrov, R. Abagyan, and K. J. Breslauer, J. Mol. Biol., **260**, 588 (1996).
[41]J. K. Myers, C. N. Pace, and J. M. Scholtz, Protein Sci. **4**, 2138 (1995).
[42]J. M. Scholtz, G. R. Grimsley, and C. N. Pace, Methods Enzymol. **466**, 549 (2009).
[43]C. N. Pace, Methods Enzymol. **131**, 266 (1986).
[44]G. I. Makhatadze, J. Phys. Chem. B **103**, 4781 (1999).
[45]M. M. Santoro, Y. F. Liu, S. M. A. Khan, L. X. Hou, and D. W. Bolen, Biochemistry **31**, 5278 (1992).
[46]E. J. Guinn, L. M. Pegram, M. W. Capp, M. N. Pollock, and M. T. Record, Jr., Proc. Natl. Acad. Sci. U. S. A. **108**, 16932 (2011).
[47]M. W. Capp, L. M. Pegram, R. M. Saecker, M. Kratz, D. Riccardi, T. Wendorff, J. G. Cannon, and M. T. Record, Biochemistry **48**, 10372 (2009).
[48]R. C. Diehl, E. J. Guinn, M. W. Capp, O. V. Tsodikov, and M. T. Record, Jr., Biochemistry **52**, 5997 (2013).
[49]E. J. Guinn, J. J., Schwinefus, H. K. Cha, J. L. McDevitt, W. E. Merker, R. Ritzer, G. W. Muth, S. W., Engelsgjerd, K. E. Mangold, P. J. Thompson, M. J., Kerins, and M. T. Record, Jr., J. Am. Chem. Soc. **135**, 5828 (2013).